

1 **THE PERFORMANCE OF FIBER REINFORCEMENT IN COMPLETELY**
2 **DECOMPOSED GRANITE**

3 **B.N. Madhusudhan^{1*}, B.A. Baudet², P.M.V. Ferreira³ and P. Sammonds⁴**

4 ^{1*}Research Fellow, University of Southampton, UK, SO17 1BJ; mbnm1f13@soton.ac.uk;
5 formerly, Post-doctoral Researcher, The University of Hong Kong, Hong Kong

6 ²Lecturer, University College London, UK, WC1E 6BT; formerly, Assistant Professor, The
7 University of Hong Kong, Hong Kong

8 ³ Lecturer, University College London, UK, WC1E 6BT;

9 ⁴Professor of Geophysics, University College London, UK, WC1E 6BT;

10

11 **Abstract**

12 Adding discrete fibers to soils can improve their strength, however fiber reinforcement remains
13 scarce in practice. Previous studies on the performance of soils reinforced with discrete fibers
14 consist mainly of laboratory studies with either clay or, most often, uniform sand as the host
15 soil, so that there is a lack of data on other types of soils such as weathered soils, which tend
16 to be well graded. Unlike uniform soils, which are generally dilative, well graded soils usually
17 show a contractive behavior. This study examines the effect of adding fibers to a completely
18 decomposed granite (CDG) typical of many residual soils which has the characteristics to be
19 sensitive to material and sample preparation and also to be compressive during shearing. It is
20 found that adding discrete fibers to the CDG homogenizes it as the reinforced soil is not
21 sensitive to the method of material or sample preparation. It is also found that despite its
22 compressive nature, fibers mobilize extra strength compared to the unreinforced soil, and this
23 effect does not reduce at large confining stresses.

24

25 **Keywords:** residual soils; reinforced soils; laboratory tests

1 **Introduction**

2 The large body of work on the potential use of fibers to improve the performance of soils
3 consists mainly of laboratory tests or constitutive modelling (e.g. Maher and Gray, 1990;
4 Maher and Ho, 1994; Michalowski and Cermak, 2003; Silva dos Santos et al., 2010; Ajayi et
5 al., 2015; Diambra and Ibraim, 2015), and seldom in-situ application (e.g. Gregory, 2011).
6 Including discrete fibers to a soil has proved to have a favorable effect on the soil's mechanical
7 properties (e.g. Consoli et al., 2005; Gray and Ohashi, 1983; Maher and Gray, 1990; Silva dos
8 Santos et al., 2010 and references that follow). The performance of fiber-reinforced soils is
9 dependent on establishing an optimum dosage of the fibers for the given soil. The increase in
10 strength is generally proportional to the quantity of reinforcement, but a limiting content is
11 usually reached when an optimum number of fibers that participate actively in the fiber-soil
12 mixture behavior is reached (Gray and Al-Rafeai, 1986). Beyond that limiting content there is
13 no significant increase in strength. Zornberg (2005) found that in both clay and sand, adding
14 fibers between 25 mm and 50 mm, in percentages of 0 to 0.4% by weight, contributes to
15 increasing the peak strength. Optimizing a fiber type and quantity is difficult, and he found that
16 at low fiber contents, fibers with a higher aspect ratio could provide the same performance as
17 fibers with a lower aspect ratio.

18 Using uniform sand as host soil (e.g. Consoli et al., 2005; Silva dos Santos et al., 2010;
19 Diambra et al., 2013) offers the advantage that it is simple to characterize (single mineralogy,
20 uniform size), with a well-defined behavior in compression and shearing so that patterns of
21 behavior associated solely with fiber reinforcement can be more easily identified. Some studies
22 were performed on sands with various gradations (e.g. Maher and Gray, 1990), or clay (e.g.
23 Maher and Ho, 1994; Ghazavi and Roustaie, 2010), highlighting the effect of the soil particle
24 size distribution, particle shape and cohesion on the fiber reinforcement. Some researchers did
25 study the performance of discrete fibers added to their local soil, for example Consoli et al.

1 (2003) or Heineck et al. (2005) used a residual sandstone from Brazil as the host soil, but its
2 non-convergent behavior (refer to Ferreira and Bica, 2006) hindered any characterization
3 within a recognized framework such as the Critical State framework, and therefore made it
4 difficult to distinguish clearly the effects of the fibers alone. Later on, the same researchers
5 switched to using a uniform sand that would allow studying the fundamental behavior of the
6 reinforced soil within the Critical State framework (e.g. Consoli et al., 2005). The behavior of
7 uniform sand reinforced with discrete fibers is now better established but it is unclear whether
8 the framework determined, for example, by Silva dos Santos et al. (2010), applies to other types
9 of soils such as weathered soils, well graded soils or larger-scale railway ballast (e.g. Ajayi et
10 al., 2015). This study used completely decomposed granite from Hong Kong (CDG) as host
11 soil, a weathered soil which has the characteristics to be sensitive to material and sample
12 preparation and also to be compressive during shearing. It will be shown, using compression
13 and shearing test data analyzed within the Critical State framework, that adding discrete fibers
14 to the CDG homogenizes it as the reinforced soil is not sensitive to the method of material or
15 sample preparation. It will also be shown that despite the compressive nature of the CDG, fibers
16 mobilize extra strength compared to the unreinforced soil, and this effect does not reduce at
17 large confining stresses.

18 The host soil used here is similar to many residual soils encountered in Europe (Viana
19 da Fonseca et al., 2006), Asia (Lee and Coop, 1995) and America (Ferreira and Bica, 2006).
20 The main characteristic is the well-graded particle size distribution with a non-negligible fines
21 content. Unlike uniform sands, which are dilative at low to medium pressures, well-graded
22 CDG displays contractive behavior from low stress levels. Given that fibers are thought to work
23 predominantly in tension (e.g. Consoli et al., 2005; Diambra and Ibraim, 2015), using them in
24 a compressive soil will bring more insight about their mechanics of reinforcement. Particular
25 to the host soil chosen, is how the effect of sample preparation, which is pronounced in the

1 unreinforced CDG (Madhusudhan and Baudet, 2014), affects the reinforcement. Like in many
2 studies on granular soils (e.g. Coop and Lee, 1993; Altuhafi et al., 2010; Silva dos Santos et
3 al., 2010), the data presented extend beyond the applicable engineering stress range so that
4 recognizable features of critical state soil mechanics, such as normal compression and critical
5 state lines, could be identified to provide a platform for comparison with other unreinforced
6 and reinforced soils and future modelling.

7 **Materials, procedures and testing apparatus**

8 Oedometer and triaxial tests were performed on specimens of completely decomposed granite
9 from Hong Kong with and without fiber reinforcement. The material used and the different
10 methods of preparation adopted are described below.

11

12 *Materials*

13 The completely decomposed granite (CDG) was obtained at Mt. Beacon, Kowloon Tong, Hong
14 Kong. It is a well-graded soil, with about 20% fines and a plasticity index of 16%. The
15 mineralogy of the soil, analyzed through EDX measurements, consists of potassium feldspar,
16 quartz and mica, with some kaolinite present in the clay fraction. In its natural disturbed state,
17 the soil consists of weakly bonded clusters of particles ranging from coarse sand to clay which
18 can be easily broken down. The maximum dry density determined by Proctor compaction is
19 18.91 kN/m^3 for an optimum water content of 11%.

20 Polypropylene fibers, similar to those used by Silva dos Santos et al. (2010), were
21 utilized to enable comparisons with the performance of a uniform sand reinforced with the
22 same type of fibers. These fibers are chemically inert and have uniform characteristics, with a
23 specific gravity of 0.91, a tensile resistance of 120 MPa, an elastic modulus of 3 GPa and a
24 range of linear deformation at rupture between 80% and 170%. The fibers, 0.023 mm diameter,

1 are manufactured as clusters and, before each test, the required amount of fibers was immersed
2 in a water-filled container where a slow-speed egg blender was activated for about 10 minutes,
3 ensuring the separation of the fibers. Two fiber lengths, 24 mm and 50mm, and two fiber
4 contents, 0.1% and 0.3% by weight, were selected. Previous studies used fibers lengths
5 between 24 and 50 mm and up to 0.9 % fibers by weight, with many studies using 0.5% by
6 weight of 24 mm fibers (e.g. Heineck et al., 2005; Silva dos Santos et al., 2010; Diambra et al.,
7 2013). Preliminary work with the CDG showed that dosages higher than 0.3% made it difficult
8 to create homogeneously reinforced specimens as the fibers occupied too much of the specimen
9 volume.

10 Material preparation:

11 The soil collected was prepared according to the specifications below:

12 Hand Destructuration (**D**): The soil samples collected were destructured by hand until all
13 particles passed through a 5mm sieve.

14 Fines reconstitution (**F**): The fines were separated from the hand destructured CDG by wet
15 sieving through a 63 μm sieve. Once the soil and the fines removed were air-dried, they were
16 mixed together in the original proportions.

17 Sample preparation:

18 Moist-tamped (**M**): The soil and the separated wet fibers were thoroughly mixed by hand at the
19 optimum water content of 11 %, until a homogeneous mixture was achieved. The mixture was
20 placed directly onto the triaxial pedestal using the under-compaction method proposed by Ladd
21 (1978) to create loose specimens. Dense specimens were prepared by tamping the soil carefully
22 using a 76 mm diameter compaction mold. The specimen was later flushed with de-aired water
23 and allowed to dry in the oven for 24 hours at 50°C. Both the loose and dense samples were
24 moist-tamped in five layers to achieve the target density (Ladd, 1978). Because of the

1 significant volume changes that typically occurred before saturation, due to macro-voids, the
2 initial dimensions were recorded after saturation by CO₂ and de-aired water flushing while
3 maintaining a small suction (<20kPa) (Madhusudhan & Baudet, 2014; Yan & Li, 2012). This
4 method was applied to both soil prepared by hand destructure and soil prepared by fines
5 reconstitution (which will be referred to in the test identification as MD and MF respectively,
6 see detail later).

7 Slurry (**S**): The soil and fibers were well mixed at a water content close to the liquid limit. For
8 loose specimens, the slurry was deposited directly into a mold on the triaxial pedestal. A small
9 suction was applied overnight using a burette placed 1m below the pedestal. For dense
10 specimens, dead weights were placed on the soil inside of the mold to reach a target density.
11 This normally took around six hours. This method was applied to the hand destructured soil
12 (noted as SD in the test identification, see detail later).

13 Dry Deposition (**D**): Hand destructured soil was sieved through 5mm sieve and deposited using
14 a hopper of 20 mm neck at zero falling height into the mould to prepare loose specimens. For
15 medium dense specimens, the soil was dry deposited and lightly tamped into appropriate split
16 mould. It was then flushed with distilled water and oven-dried for 24 h at 50°C, in order to
17 eliminate macro-voids without the problem of segregation. The oven dried cylindrical
18 specimens were then transferred to the triaxial pedestal and saturated by carbon dioxide (CO₂)
19 followed by de-aired water circulation under a suction of 20 kPa. Those specimens are referred
20 in the test identification as DD (see detail later).

21 *Testing procedures and apparatus*

22 The testing program was designed so as to emphasize the effect of the material preparation, the
23 fiber type and dosage and the added performance when compared to the unreinforced soil. The
24 first series of tests consisted of triaxial tests on 76 mm diameter specimens to compare the

1 effects of fiber length and fiber quantity: type A – fiber length of 24mm and fiber content of
2 0.3%; type C – fiber length of 50mm and fiber content of 0.3%; type D – fiber length of 50mm
3 and fiber content of 0.1% (Table 1). Ang and Loehr (2003) showed that 70 mm specimens used
4 with 50 mm fibers (i.e. a ratio of 1.4 between specimen size and fiber length) were
5 representative of the larger reinforced soil mass. Once the optimum fiber mixture of 24 mm
6 and 0.3% was determined, compression was investigated primarily via oedometer tests, whilst
7 shearing was investigated via standard (76 mm diameter) and high pressure (38 mm diameter)
8 triaxial tests. For these tests on smaller specimens, the ratio between specimen diameter and
9 fiber length is about 1.5, which is typical in studies on fiber-soil mixtures (e.g. Silva dos Santos
10 et al., 2010; Diambra et al., 2013), and is also consistent with the ratio of 1.4 used by Ang and
11 Loehr (2003).

12 In Table 1, the test identification is given in the first column, which contains details
13 about the material and sample preparation: reinforced (R)/unreinforced (U), the type of fiber
14 combination (A, C or D), sample number (1 or 2), sample preparation (M, S or D), material
15 preparation (D or F) and the effective stress at which the sample was sheared. Samples MD,
16 i.e. hand destructured and moist tamped, were thought to represent best the in-situ compaction,
17 whilst samples prepared using SD (i.e. hand destructured and made into a slurry) and MF (i.e.
18 made by fines reconstitution and moist-tamping) are believed to represent better the extreme
19 weather conditions during the rainy season, when the fines may become separated from the
20 coarse soil grains.

21 Triaxial testing: Undrained and drained compression tests were carried out on specimens of 76
22 mm diameter and 152 mm height, using a standard triaxial apparatus mounted on an automated
23 loading frame. Normally consolidated specimens were tested under effective confining stresses
24 of 50, 100 kPa, 200kPa and 500 kPa while a few over-consolidated specimens were tested

1 under confining stresses of 50, 100 and 200 kPa. The cell pressure and back pressure (applied
2 at the bottom of the specimen) were monitored with GDS controllers of 2 MPa capacity, and
3 the axial strains were measured by an external displacement transducer. The shear strain was
4 calculated as $\epsilon_s = \epsilon_a - 1/3 \epsilon_v$, with ϵ_a and ϵ_v being the axial and volumetric strains. The pore
5 water pressure was measured at the top of the specimens. Precautions were taken to reduce the
6 friction between the end platens and specimen by using smaller porous stones flush with the
7 platens. Each specimen was covered by two latex membranes smeared with room temperature
8 vulcanizing silicon rubber coating wherever sharp edges were felt. Appropriate membrane
9 corrections were applied (Head, 1980). The specific volume was obtained by four expressions
10 using independent variables such as the initial and final weights and volumes of the soil
11 specimen, following the method described in Madhusudhan and Baudet (2014). The difference
12 between the maximum and minimum initial specific volumes, calculated in this way, is
13 reported in Table 1 as specific volume precision. The average precision was 0.023 for both the
14 reinforced specimens and the unreinforced CDG. The fibers were considered as solids in the
15 calculations. The specific gravity of the fiber-CDG mixture was taken equal to that of the
16 unreinforced CDG, which was determined in laboratory to be 2.65, as it was found that the
17 effect of adding 0.3% fibers or less by weight had a negligible influence on the specific gravity
18 (less than 1%) and on the specific volume (less than 0.02). The summary of the tests and
19 accuracy of the specific volumes are given in Table 1, where v_0 refers to the initial specific
20 volume, v_c refers to the specific volume before shearing and HP identifies the triaxial tests that
21 were carried out at high pressures.

22 Complementary high pressure triaxial compression tests were carried out on specimens
23 prepared with 24 mm fibers, at University College London, using an apparatus described in
24 Altuhafi et al. (2010), capable of reaching pressures up to 20 MPa. The specimens tested had
25 38 mm diameter by 76 mm height and were prepared using the moist-tamping and slurring

1 methods. For these tests, the puncture of the membrane was avoided by using two neoprene
2 membranes. Details about these tests are also presented in Table 1.

3 Oedometer testing: Some specimens prepared with 24 mm fibers were tested in one-
4 dimensional compression using a floating ring oedometer cell of 38mm diameter and 25mm
5 height. The specimens were created directly into the oedometer cell after smearing its inner
6 surface with a thin layer of silicon grease. They were then saturated in a water bath for 12-15
7 hours before compression to 15 MPa for the moist-tamped specimens and 24 MPa for the
8 slurried ones. The initial specific volume was calculated by four different methods that made
9 use of the initial height of the specimen, measured by calliper and by dial gauge (resolution
10 0.01 mm), and the final height (see Madhusudhan and Baudet, 2014). The results presented are
11 for tests in which the void ratios calculated with the four methods fall within a range of ± 0.01 .

12 **Selection of fiber-CDG mixture**

13 A comparison of the performance of the three fiber combinations (A, C and D) in shearing is
14 shown in Figure 1, using data from reinforced and unreinforced specimens sheared from similar
15 void ratios for a given confining stress (Table 1). Plain lines are used for the reinforced
16 specimens and dashed lines for the unreinforced ones. The sample preparation methods are
17 differentiated by using open symbols for moist-tamping and closed symbols for fines
18 reconstitution or slurry, although it will be shown later that the sample preparation does not
19 affect the results of the reinforced specimens in the same way as it does for the unreinforced
20 soil. A first observation is that the specimens with a fiber content of 0.1% (type D; specimens
21 RD1MD100 and RD1MF500) show no improvement on the strength for any material or sample
22 preparation method. The specimens prepared with 0.3% of 24 mm fibers (type A) show the
23 best performance, with the strength multiplied by about 2.3 at low pressure (RA1MD100).
24 Specimen RA1SD500 reaches a lower stress ratio but it will be shown later that it is not due to

1 the higher confining stress but is more likely to be test specific. Using longer fibers of 50 mm
2 (RC1SD100) does not add any benefit to the reinforced soil strength. The method of
3 preparation does not seem to affect the strength, the curves for specimens RA1MD100 and
4 RC1SD100 plotting close to each other. The performance of the fibers is particularly significant
5 after 10% shear strain, where additional strength is gained until a critical state is reached.

6 Based on the stress dilatancy graph shown in Figure 1b, it is observed that the inclusion
7 of fibers makes the volumetric response more contractive during tests at low confining stress
8 (when compared to the unreinforced specimen URSD100), whilst no significant change is
9 noticed for higher stress levels. The unreinforced (URDD500) and reinforced specimens follow
10 the same stress dilatancy path at the start of the tests, showing that the current strength is
11 mobilized as compressive volumetric strains develop. The unreinforced specimens reach
12 critical state at a stress ratio $M = 1.57$. The paths of the fiber-CDG mixtures become steeper
13 from about $d\varepsilon_v/d\varepsilon_s=0.2$ as the fiber reinforcement becomes effective at large deformation,
14 possibly owing to lock-in of the fibers between grains as the particles re-arrange. As observed
15 in the stress-strain curves, the type-D fiber combination, which only contains 0.1% fiber, leads
16 to the lower strength with a stress ratio M at critical state of 1.83, while the specimens with a
17 higher fiber content of 0.3% reach values $M = 2.25$ for 24 mm fibers (type A) and $M = 1.83$
18 for 50 mm fibers (type C). The steepening of the stress dilatancy path towards critical state
19 concurs with the late increase in strength observed in Figure 1a, at about 10% shear strain,
20 which also marks the beginning of different stiffnesses. Based on these results, the research
21 then focused on investigating the behavior of type-A mixtures (i.e. with 0.3% of 24 mm fibers)
22 and comparing it with that of the unreinforced soil.

23 **Compression behavior**

24 The location of the normal compression line (NCL) of the unreinforced CDG is sensitive to the
25 method of material and sample preparation, with the NCL of specimens prepared by fines

1 reconstitution or by hand destructure and slurry lying above that of specimens prepared by
2 hand destructure and moist-tamping (Madhusudhan and Baudet, 2014). The influence of
3 the material and sample preparation method is evident in both one-dimensional and isotropic
4 normal compression lines (Fig. 2). Figure 2a shows the compression data obtained from
5 oedometer tests; the curves for the unreinforced specimens prepared by fines reconstitution or
6 by hand destructure and slurry (open circles) converge to a line distinctly separate from the
7 curve reached by the unreinforced specimens prepared by hand destructure and moist-
8 tamping or dry deposition (open diamonds). Washing the CDG or using a large amount of
9 water in the sample preparation displaces the particles, creating fabrics that can reach higher
10 values of mean effective stress. In contrast, the curves for the fiber-reinforced specimens, which
11 were all prepared by hand destructure and are represented by closed symbols, converge to
12 a unique normal compression line irrespective of whether the samples were made by moist-
13 tamping or by the slurry method.

14 Additional K_0 -compression and high pressure isotropic compression tests, performed
15 in the triaxial apparatus, show the same pattern (Figure 2b). The reinforced CDG does not seem
16 to be affected by the method of preparation, as if the fibers acted as a homogenizer for the soil.
17 A positive reinforcing effect with a higher strength at a given void ratio is observed when
18 compared to the unreinforced MD specimens, with the isotropic normal compression line (iso-
19 NCL) of the reinforced specimens plotting parallel and above that of the reconstituted
20 specimens. No such improvement is observed when comparing with the unreinforced
21 specimens prepared by fines reconstitution or by slurry (MF or SD). It has been suggested from
22 test results on moist-tamped samples that fibers assist the agglomerates in resisting the
23 compressibility by lock-in of the fibers between sand grains (Consoli et al., 2005). In the
24 reinforced specimens prepared by fines reconstitution or hand destructure and slurry, the
25 larger amount of fine particles free to move in the specimens does not seem to influence the

1 location and slope of the NCL, suggesting that there may be an overriding effect of the fiber
2 lock-in between coarse particles, creating a unique compression curve for the fiber-soil mixture
3 whatever the method of material or sample preparation.

4 The compression parameters determined for the fiber-CDG mixture are summarized in
5 Table 2. The parameters for the normal compression lines of the unreinforced CDG, also given
6 in Table 2, were determined by Madhusudhan and Baudet (2014). For moist-tamped specimens,
7 the effect of adding fibers is similar to what was found by Silva dos Santos et al. (2010) on
8 quartzitic sand.

9 **Shearing behavior**

10 Normally and over-consolidated specimens of reinforced CDG were sheared drained or
11 undrained in the triaxial apparatus, most specimens being 76 mm diameter while the high
12 pressure tests were carried out on 38 mm diameter specimens. Typical stress-strain-volume
13 responses are presented in Figure 3, in terms of stress ratio (Fig. 3a) and stress dilatancy (Fig.
14 3b). As in Figure 1, the curves for the reinforced specimens are represented by plain lines while
15 for unreinforced specimens dashed lines are used, material and sample preparation methods are
16 differentiated by using open symbols for hand destructure and moist-tamping; closed
17 symbols are used for fines reconstitution or hand destructure and slurry.

18 The unreinforced specimens almost all reach a stable stress ratio of 1.57 at large strains
19 (Fig. 3a). The reinforced specimens reach a much higher stress ratio, including those tested
20 under very high confining pressures (RA MD HP and RA SD HP), which were stopped at
21 strains around 15% because of the displacement capacity of the apparatus, at which strain level
22 the stress ratio and volumetric deformations had stabilized or were showing signs to stabilize.
23 This suggests that there is no loss of efficiency of the fibers with increasing stress, unlike what
24 was found in other soils (e.g. Maher and Gray, 1990; Silva dos Santos et al., 2010). Particular

1 to the CDG, this seems to apply whatever the method of preparation (moist tamping or slurry).
2 Two specimens did reach lower stress ratios (RA1MD 200 and RA1SD 500) but given that
3 they were prepared with different methods (MD and SD) and tested at medium pressures, this
4 cannot easily be attributed to either the sample preparation method or the confining stress and
5 is more likely to be an unusual feature of these two tests.

6 The stress dilatancy plotted in Figure 3b sheds more light on the development of the
7 strength. As noted above, all the unreinforced specimens reach critical state at a stress ratio M
8 $= 1.57$. The reinforced specimens reach critical state at higher stress ratios generally greater
9 than $M = 1.90$, and their path becomes steeper from about $\delta\varepsilon_v/\delta\varepsilon_s=0.2$. The data for the high
10 pressure tests are a bit more scattered but they seem to follow the same tendency. There is
11 however a difference with the behavior of reinforced uniform quartzitic sand such as that tested
12 by Silva dos Santos et al. (2010), for which an upwards “tail” in the stress dilatancy is seen,
13 which indicates a very rapid increase in strength with dilation.

14 Another difference with uniform quartzitic sands, which require strains much larger
15 than those typically reached in triaxial tests to reach a true critical state (e.g. Coop et al., 2004;
16 Muir Wood, 2006), is that while they only reach the steep, linear part of the NCL and CSL
17 (defined as $v = N - \lambda \ln p'$ and $v = \Gamma - \lambda \ln p'$ respectively) at very high stresses, when particle
18 breakage is occurring, well-graded residual soils such as CDG can reach their NCL and true
19 critical state at lower stresses and strains, as seen in Figures 1 and 3. This was also reported by
20 Santucci et al. (1998) and Ferreira and Bica (2006) for silty sand and residual soil. Here critical
21 state was identified as the point at which the stress ratio (q/p') and/or volumetric strain becomes
22 constant, which in most tests - except the high pressure tests - occurred at strains larger than
23 30% (Figure 3a).

1 The critical state line for the unreinforced CDG was determined from the stress
2 dilatancy plot in Figure 3b to have a gradient $M = 1.57$. Madhusudhan and Baudet (2014) found
3 that it is unique and not influenced by the method of preparation. The performance of the fiber-
4 reinforced soil can be assessed by comparing the strength of the reinforced specimens with the
5 critical state strength of the corresponding unreinforced CDG specimens. The end-of-test
6 points, most of them at critical state, are reported in Figure 4a (low stress levels) and Figure 4b
7 (high stress levels). At low stress levels, the data points for the reinforced specimens plot above
8 the critical state line for the unreinforced CDG, forming an almost straight line of slope $M =$
9 1.90 , which corresponds to the lower bound value found from the stress dilatancy data in Figure
10 3b. When the critical state lines are extended to high pressures (Figure 4b), the effect of the
11 fiber reinforcement in providing additional strength to the host soil remains even at deviatoric
12 stress levels greater than 100MPa.

13 Maher and Gray (1990), who tested well graded sands as well as uniform sands,
14 suggested a bilinear failure envelope, with a critical pressure delimiting the pressure range
15 when the fibers may be slipping (low confining stresses) and when they may be resisting pull-
16 out by stretching (high confining stresses), the latter resulting in a failure envelope above and
17 parallel to that of the unreinforced soil. They tested soils up to 500 kPa confining stress and
18 found that well graded sands had a lower critical pressure than uniform sands, and a higher
19 contribution to the strength from the fibers. Their model suggests that the fibers contribute less
20 to the resistance as confining stress levels increase. Silva dos Santos et al. (2010), who
21 performed high pressure tests similarly to this study, had found for a reinforced uniform
22 quartzitic sand that the critical state line is curved, and tends to converge to that of the
23 unreinforced sand at large stresses. Diambra and Ibraim (2015) also found, from analytical
24 studies, that larger tensile stresses are mobilized in fibers as the soil becomes stiffer at large
25 confining stresses. Here, the fibers tested at high confining stress contribute the same amount

1 of strength as those tested at lower pressures (Fig. 3a), about 20%, which is of the order of 20
2 MPa for the high pressure tests. With an elastic modulus of 3 GPa, this would cause only a
3 small amount of deformation in the fibers. Visual inspection of the fibers after a high pressure
4 test showed that a significant but not extensive number of fibers had broken, and this may also
5 have happened during isotropic compression (Silva dos Santos et al., 2010), although fiber
6 breakage in uniform soil is also caused by nipping, which is less likely in well graded soils. It
7 may also be that the very large stiffness of the fibers compared to that of the CDG allows the
8 large stresses to be taken, while in stiffer soils like quartzitic sands the fibers reach their
9 maximum elongation more rapidly.

10 The K_0 triaxial compression stress paths of the reinforced and the unreinforced CDG,
11 plotted in Figure 4a, show clearly that each unreinforced sample preparation method has a
12 different value of earth pressure at rest, $K_0 = 0.40$ for the slurried specimen and $K_0 = 0.46$ for
13 the specimen prepared by dry deposition. This may have been caused by the removal of the
14 fines coating of the coarse grains during washing or preparation by slurry, rendering the soil
15 grains rougher and possibly affecting the friction angle. The addition of fibers cancels this
16 effect, the K_0 stress paths of the reinforced specimens tested with different preparation methods
17 are the same, regardless of the method of preparation, and almost coincident with that of the
18 slurried unreinforced specimen, as shown in Figure 4a.

19 The state paths for all the tests on reinforced specimens tested at low to medium
20 pressures are shown in a plot of specific volume, v , against the logarithm of the mean effective
21 stress, $\ln p'$, in Figure 5. When the volumetric response did not reach a stable state, which
22 occurred sometimes in the reinforced soil, when the stress exceeded the load cell capacity, if
23 there was not enough length for the piston to be able to complete the test, or when the tests
24 were stopped at the onset of the shear plane development, the test end points and the direction
25 of the state paths were noted and they are reported with arrows. A unique critical state line can

1 be defined for the fiber-reinforced CDG regardless of the preparation method involved (refer
2 to Table 1). The end-of-test points of the reinforced specimens, found mostly to be at critical
3 state, are replotted in Figure 6 without the state paths for clarity. The high pressure data points,
4 also plotted in Figure 6, are not aligned with the log-line part of the CSL and seem to indicate
5 a much shallower slope. This may be because at those high stresses very low void ratios (close
6 to zero) are reached, since negative void ratios are not possible, the void ratios at critical state
7 may tend to converge to a low value.

8 While two distinct CSLs were found for the unreinforced soil, which depend on the
9 preparation method (Madhusudhan and Baudet, 2014), a unique CSL can be identified for the
10 reinforced CDG, parallel to the CSLs of the unreinforced soil. As was found earlier for the
11 compression behavior, the addition of fibers seems to act as homogenizer and to cancel the
12 effect of the preparation method in the volumetric response. Ekinici and Ferreira (2012) also
13 found that adding fibers to clay changes the mode of failure by inhibiting the formation of a
14 shear plane. As pointed out earlier, the critical state and normal compression lines do not seem
15 to curve at lower pressures for either unreinforced or reinforced soil (Fig. 6), and the distance
16 between the CSL and NCL appears to be similar for both unreinforced and reinforced
17 specimens. The slopes and intercepts of the critical state lines are reported in Table 2, using,
18 for the unreinforced CDG, the values that were determined by Madhusudhan and Baudet (2014).
19 Similarly to what was found for the NCL, the CSL of the reinforced soil coincides with that of
20 the unreinforced specimens prepared by moist tamping and fines reconstitution (MF) or hand
21 destructuration and slurry (SD). The NCL and CSL of the MD specimens are above the lines
22 determined for the unreinforced CDG prepared with the same method, at a vertical distance of
23 about 0.03 (within an error margin of ± 0.01).

24 The effect of the fiber reinforcement on the size of the state boundary surface can be
25 determined by normalizing the triaxial stress paths for volume, by using an equivalent pressure

1 on a reference line in v - $\ln p'$ space (Figure 7). Figure 7a identifies the state boundary surface of
2 the unreinforced CDG and Figure 7b the surface for the reinforced CDG. The CSL is taken
3 here as the reference line, using the appropriate CSL corresponding to the reinforced CDG and
4 unreinforced CDG, either MD/DD or SM/MF as relevant, to determine the equivalent pressure
5 $p_{cs}' = \exp\left(\frac{\Gamma - v}{\lambda}\right)$, with the values of Γ and λ as determined in Table 2. The different values of
6 M for the reinforced and unreinforced CDG explain the shift of the normalized critical state
7 line (plotted as a point) upwards for the fiber-CDG. With the type of normalization applied, the
8 stress paths for the reinforced CDG plot within the state boundary surface for the unreinforced
9 CDG. Some hand destructured and slurried specimens (SD), both reinforced and unreinforced,
10 only joined the iso-NCL at large stresses so for the triaxial compression tests at low confining
11 stress the value of p'/p'_{cs} at the start of shearing can be as high as 3.0.

12 **Further insight on the mechanics of the fiber-CDG mixture**

13 Effect of overconsolidation

14 A series of drained tests was performed to investigate the effect of overconsolidation on the
15 performance of the CDG reinforced with type-A fibers. Two over-consolidated (OC)
16 specimens with an overconsolidation ratio $OCR = 6$ were sheared from $p' = 50$ and 100 kPa
17 and one with an OCR of 3 was tested from $p' = 200$ kPa. The test results obtained from these
18 specimens can be compared with the normally consolidated (NC) specimens sheared at $p' = 50$,
19 100 and 200 kPa already presented above. It was difficult to obtain the same void ratio for the
20 NC specimens and their corresponding OC specimens, but a comparison can be made by taking
21 account of the state of the specimens, summarized in the inset on Figure 8a, which shows the
22 specimen initial states prior to shearing. Because of the large stresses required to reach the
23 NCL, none of the “normally consolidated” specimens lie on it at the start of shearing, however,

1 apart from specimen RA2MD50, they plot to the right of the CSL and therefore should display
2 a contractive behavior upon shearing. All three overconsolidated specimens are on the “dry”
3 side of critical (i.e. to the left of the CSL) and are expected to dilate upon shearing.

4 Figures 8a and 8b show the stress-strain and volumetric responses respectively, the
5 overconsolidated specimens being represented by open symbols. It is obvious from Figure 8a
6 that the overconsolidated specimens reach a lower deviatoric stress at failure than the normally
7 consolidated specimens sheared at the same confining pressure, by 75% at the low confining
8 stress of 50 kPa, the difference reducing to 8% at the higher confining stress of 200 kPa. They
9 also display a more dilative behavior (Fig. 8b), which can be predicted from their initial state
10 on the “dry” side of critical. Two specimens starting from comparable states slightly to the left
11 of the CSL, RA2MD50 (OCR = 1) and RA1SD200 (OCR = 3), show the same amount of
12 volumetric deformation. Only specimen RA1MD200 displays unexpected dilative behavior
13 considering the high initial void ratio, which may be attributed to some localization within the
14 specimen. It was also highlighted above for behaving unusually and reaching a lower strength
15 than expected (Fig. 3a). The OC specimens have a high initial stiffness, mobilizing their
16 strength rapidly from low strains. The stress dilatancy shown in Figure 8c emphasizes that rapid
17 gain in strength in the overconsolidated specimens with almost no volumetric deformation up
18 to the peak stress ratio while the normally consolidated specimens follow a path typical of
19 frictional materials, compressing to the maximum value of q/p' . The value of q/p' at critical
20 state is much less for the OC specimens, with $M = 1.75$, than for the NC specimens which
21 reached $M = 2.25$. It is interesting that against preconceptions that fibers should be mobilizing
22 tensile resistance when shear strains develop, when comparing with the OC specimens, which
23 tend to dilate, the NC specimens (which contract upon shearing) reach higher strengths. It
24 therefore seems that tensile strains are not the only requirement for fibers to mobilize strength,
25 and that their complex orientation within the specimen combined with the continuous particle

1 rearrangement during shearing contribute with a non-negligible part to the resistance.
2 Unfortunately, unless experimental micromechanical studies of the fiber-soil interaction
3 mechanism are made it is difficult to be certain about this.

4 Fiber-soil grains interaction

5 The CDG, which contains about 20% fines, behaves differently when the sample preparation
6 method involves a large amount of water (e.g. by making a slurry), which may separate the
7 fines attached to the coarse particles by light cementation than it does when prepared dry or
8 moist-tamped. The main effect is a shift in the locations of the NCL and CSL in the v - $\ln p'$ plane
9 (e.g. Fig. 2, 6). It has been shown that unlike for the unreinforced CDG, adding fibers seems to
10 lead to a more homogenous response with unique critical state and normal compression lines,
11 independently of the fines free to move in the soil matrix. In the q - p' plane, the well-graded
12 nature of the soil also seems to make the fibers effective even at very large stresses (Figure 4),
13 unlike what is usually found or hypothesized for fiber-soil mixtures (e.g. Maher and Gray,
14 1990; Silva dos Santos et al., 2010). The contribution of clay particles to the bonding and
15 friction between soil and fibers was shown by Tang et al. (2007) who combined single fiber
16 pull out tests in small samples of clayey silt with scanning electron microscopy. Tang et al.
17 (2016) also showed that coarse grains can increase the roughness of the fibers by plowing and
18 thus their interlocking strength. Monitoring the particle breakage in the specimens may provide
19 further insight into the fiber-soil interaction: Silva dos Santos et al. (2010) showed how a
20 significant amount of fibers break during isotropic compression to high stresses, some of them
21 possibly by nipping, and further are broken during shearing. The specimens were sieved before
22 and after the drained high pressure triaxial tests (Figure 9). As was found by Silva dos Santos
23 et al. (2010) for uniform sand, the unreinforced specimens suffered more breakage than the
24 reinforced ones. The moist-tamped specimens were the most affected. It is expected that, in

1 specimens where fines were released during the sample preparation, the higher number of
2 contacts between grains would lead to less breakage, but little difference is seen between the
3 different methods of preparation, suggesting that the fibers might have hindered the force
4 transmitting contacts between particles in all specimens. Upon examination of the fibers after
5 test, it was found that some fibers were twisted, some were elongated and a significant but not
6 extensive amount was broken, which reinforces the finding that fibers added to well graded
7 weathered soil have a potential to mobilize strength even at large confining stress.

8 **Conclusions**

9 This study showed that adding discrete fibers to a well graded completely decomposed granite
10 can improve its performance. Similarly to what was found in previous research for uniform
11 quartzitic sands, a low fiber content is enough to gain significant additional strength in the
12 reinforced soil, with values of stress ratio at critical state 20 to 40% greater than that of their
13 unreinforced counterparts. The normal compression line and critical state line of the reinforced
14 soil are parallel and above those of the unreinforced soil. The fibers also seem to reduce the
15 amount of grain breakage during compression. Two additional fundamental points that should
16 contribute to the database on fiber-soil composites have been highlighted:

17

- 18 • Fibers were found to contribute to the strength of the soil despite the compressive nature
19 of the host soil, thus showing that tensile strains are not the only requirement for fibers
20 to mobilize their strength, but that the complex combination of fiber orientation, fiber
21 stiffness and continuous particle rearrangement also contribute to the resistance.
- 22 • In completely decomposed granite, which contains a non-negligible amount of fines,
23 the method of sample preparation, in particular adding a large amount of water at the
24 stage of material or sample preparation, affects the fabric and the overall behavior, such

1 as the location of the NCL and CSL. The reinforced CDG however was found to have
2 a unique normal compression line and a unique critical state line independently of the
3 method of sample preparation, the fibers having a homogenizing effect on the mixture.

4 **Acknowledgements**

5 This research was made possible thanks to the financial support provided by the Hong Kong
6 Research Grant Council (grant GRF No.710211). The authors are also indebted to Professor
7 Nilo Consoli from the University Federal of Rio Grande do Sul for providing the fibers.

8 **References**

- 9 Ang, E.C., and Loehr, J.E. (2003). "Specimen Size Effects for Fiber-Reinforced Silty Clay in
10 Unconfined Compression". *Geotechnical Testing Journal*, 26(2), 1-10.
- 11 Ajayi, O., Le Pen, L., Zervos, A., and Powrie, W. (2016). "A behavioral framework for fibre
12 reinforced gravel." *Géotechnique*, (In Press), DOI:10.1680/jgeot.16.P.023.
- 13 Altuhafi F., Baudet B.A., and Sammonds P. (2010). "The mechanics of subglacial sediment:
14 an example of new "transitional behavior"." *Canadian Geotechnical Journal*, 47 (7),
15 775-790.
- 16 Consoli, N. C., Casagrande, M. D. T., Thomé, A. and Prietto, P. D. M. (2003). "Plate load test
17 on fiber-reinforced soil." *J. Geotech. Geoenviron. Eng.*, 129(10), 951–955.
- 18 Consoli, N.C., Casagrande, M.D.T., and Coop, M.R. (2005). "Effect of fiber reinforcement on
19 the isotropic compression behavior of a sand." *J. Geotech. Geoenviron. Eng.*, 131(11),
20 1434-1436.
- 21 Coop, M.R., and Lee, I.K. (1993). "The behavior of granular soils at elevated stresses." In:
22 *Predictive soil mechanics*, Proc. of the C. P. Wroth Memorial Symposium (Houlsby
23 and Schofield eds.), pp. 186–198. London, UK: Thomas Telford.

1 Coop, M.R., Sorensen, K.K., Bodas Freitas, T., and Georgoutsos, G. (2004). “Particle breakage
2 during shearing of a carbonate sand.” *Géotechnique*, 54(3), 157–163.

3 Diambra, A., Ibraim, E., Russell, A. R., and Muir Wood, D. (2013). “Fibre reinforced sands:
4 from experiments to modelling and beyond”. *International Journal for Numerical and*
5 *Analytical Methods in Geomechanics*, 37(15), 2427-2455

6 Diambra, A., and Ibraim, E. (2015). “Fiber-reinforced sand: interaction at the fiber and grain
7 scale.” *Géotechnique*, 65(4), 296-308.

8 Ekinci, A., and Ferreira, P.M.V. (2013). “Effects of fibre inclusion on stress strain behavior of
9 a compacted over-consolidated clay from Lambeth group.” In: Proc. Int. Conf. Ground
10 Improv. Ground Control (Indraratna et al. eds.), ICGI Wollongong 2012, pp. 912-917.
11 Singapore: Research Publishing Services.

12 Ferreira, P.M.V., and Bica, A.V.D. (2006). “Problems on the identification of structure in a soil
13 with a transitional behavior.” *Géotechnique*, 56(7), 445–454.

14 GEO Publication No.1/2011 www.cedd.gov.hk/eng/publicatios/geo/doc/ep1_2011.pdf

15 Ghazavi, M., and Roustaie, M. (2010). “The influence of freeze-thaw cycles on the unconfined
16 compressive strength of fiber-reinforced clay.” *Cold Reg. Sci. Technol.*, 6,125–131.

17 Gray, D.H., and Al-Refeai, T. (1986). “Behavior of fabric versus fiber reinforced sand.” *J.*
18 *Geotech. Eng.*, 112(8), 804-826.

19 Gray, D.H., and Ohashi, H. (1983). “Mechanics of fiber-reinforcement in sand.” *J. Geotech.*
20 *Eng.*, 109(3), 335-353.

21 Gregory, G. (2011). “Sustainability and the fiber-reinforced soil repair of a roadway
22 embankment.” *Geosynthetics Magazine*, Bouquet 08, August 2011.

23 Hall, S.A., Bornert, M., Desrues, J., Pannier, Y., Lenoir, N., Viggiani, G., and Bésuelle, P.
24 (2010). “Discrete and continuum analysis of localised deformation in sand using X-ray μ CT
25 and volumetric digital image correlation.” *Géotechnique*, 60(5), 315-322.

- 1 Head, K.H. (1980). *Manual of soil laboratory testing*, 3 vols. London, Plymouth, UK: Pentek.
- 2 Ladd, R.S. (1978). "Preparing test specimens using under-compaction." *Geotech. Testing J.*,
3 1(1): 16-23.
- 4 Lee, I.K., and Coop, M.R. (1995). "The intrinsic behavior of a decomposed granite soil."
5 *Géotechnique*, 45(1), 117–130.
- 6 Madhusudhan, B.N., and Baudet, B.A (2014). "Influence of reconstitution method on complete
7 decomposed granite soil." *Géotechnique*, 64(7), 540-550.
- 8 Maher, M.H., and Gray, D.H. (1990). "Static response of sands reinforced with randomly
9 distributed fibers." *J. Geotech. Eng.*, 116(11), 1661-1677.
- 10 Maher, M.H., and Ho, Y.C. (1994). "Mechanical properties of kaolinite/fiber soil composite."
11 *J. Geotech. Eng.*, 120(8), 1381-1393.
- 12 Michalowski, R.L., and Cermak, J. (2003). "Triaxial compression of sand reinforced with
13 fibers." *J. Geotech. Geoenviron. Eng.*, 129(2), 125-136.
- 14 Muir Wood, D. (2006). "Geomaterials with changing grading: a route towards modelling."
15 *Proc. Int. Symp. Geomech. Geotech. Particulate Media, Ube, Yamaguchi, Japan:*
16 *Geomechanics and Geotechnics of Particulate Media* (eds. M. Hyodo, H. Murata and
17 Y. Nakata), pp. 313–325. London, UK: Taylor and Francis Group.
- 18 Salvagni Heineck, K., Coop, M.R., and Consoli, N.C. (2005). "Effect of microreinforcement
19 of soils from very small to large shear strains." *J. Geotech. Geoenviron. Eng.*, 131(8),
20 1024-1033.
- 21 Santucci, F., Silvestri, F., and Vinale, F. (1998). "The influence of compaction on the
22 mechanical behavior of a silty sand." *Soils and Foundations*, 38(4), 41-56.
- 23 Silva dos Santos, A.P., Consoli, N.C., and Baudet, B.A. (2010). "The mechanics of fiber-
24 reinforced sand." *Géotechnique*, 60(10), 791-799.

- 1 Tang, C.S., Shi, B., Gao, W., Chen, F., and Cai, Y. (2007). “Strength and mechanical behavior
2 of short polypropylene fiber reinforced and cement stabilized clayey soil” *Geotextiles
3 and Geomembranes* 25, 194-202.
- 4 Tang, C.S., Shi, B., and Zhao, L.Z. (2010). “Interfacial shear strength of fiber reinforced soil.”
5 *Geotextiles and Geomembranes* 28, 54-62.
- 6 Viana da Fonseca, A., Carvalho, J., Ferreira, C., Santos, J.A., Almeida, F., Pereira, E.,
7 Feliciano, J., Grade, J., and Oliveira, A. (2006). “Characterization of a profile of
8 residual soil from granite combining geological, geophysical and mechanical testing
9 techniques.” *Geotech. Geol. Eng.*, 24, 1307-1348.
- 10 Yan, W.M, and Li, X.S. (2012). “Mechanical response of medium-fine-grained decomposed
11 granite in Hong Kong.” *Eng. Geol.*, 129-130, 1-8.
- 12 Zornberg, J.G. (2005). “Advances in Reinforced Soil Technology.” *Proc. Int. Symp. Geosynth.
13 Applications Ground Reinforcement and Improvement*, July 6-7, Busan, South Korea,
14 pp. 155-196.
- 15

1 Table 1 - Summary of the triaxial tests performed on reinforced and unreinforced CDG.

Test	w_0 (%)	v_0	v_c	Specific volume precision	P_c' (kPa)	OCR	Method	γ_a (kN/m ³)	Test type
Type A: fiber length = 24 mm, fiber content = 0.3%									
RA2MD50	11.4	1.52	1.50	0.012	49	1	MD	17.06	CID
RA1MD100	11.0	1.66	1.51	0.011	100	1	MD	15.62	CID
RA2MD100	10.6	1.67	1.40	0.042	99	6	MD	16.41	CID
RA1MD200	11.3	1.54	1.46	0.020	203	1	MD	17.95	CID
RA1MF500	11.2	1.59	1.40	0.025	499	1	MF	16.11	CID
RA1MD K_0	11.2	1.57	1.38	0.025	635	-	MD	16.22	CK ₀ D
RAMD HP	11.0	1.53	1.18	0.02	20000	1	MD	16.95	HP CID
RA1SD50	19.8	1.52	1.42	0.018	48	6	SD	17.05	CID
RA1SD200	20.1	1.67	1.40	0.041	210	3	SD	15.97	CID
RA1SD340	20.0	1.59	1.45	0.032	341	1	SD	17.65	CID
RA1SD500	20.4	1.64	1.42	0.024	500	1	SD	16.95	CID
RA1SD750	20.3	1.65	1.36	0.038	749	1	SD	16.05	CID stress Path
RA1SD1000	20.4	1.54	1.38	0.005	984	1	SD	17.06	CID
RA2SD1000	20.6	1.60	1.37	0.025	1000	1	SD	17.45	CIU
RA1SD1200	20.5	1.55	1.35	0.010	1200	1	SD	17.28	CID
RA1SD K_0	18.4	1.53	1.34	0.015	1065	-	SD	16.78	CK ₀ U
RA SD HP	20.6	1.53	1.19	0.02	20015	1	SD	17.44	HP CID
Type C: fiber length = 50 mm, fiber content = 0.3%									
RC1SD100	20.4	1.56	1.46	0.021	98	1	SD	16.65	CID
RC1SD1350	20.3	1.62	1.37	0.025	1300	1	SD	16.23	CID

2

3

RC1SD K ₀	20.5	1.52	1.35	0.007	909	-	SD	17.21	CK ₀ U
Type D: fiber length = 50 mm, fiber content = 0.1%									
RD1MD100	11.1	1.64	1.52	0.030	97	1	MD	15.85	CID
RD1MD500	11.2	1.62	1.43	0.010	495	1	MD	15.51	CID
Unreinforced CDG (data from Madhusudhan and Baudet, 2014)									
URDD50	0.1	1.51	1.47	0.012	45	1	DD	17.06	CID
URSD100	20.3	1.58	1.46	0.021	112	1	SD	16.04	CID
URDD500	0.1	1.50	1.34	0.007	494	1	DD	17.87	CID
URMF K ₀	11.2	1.64	1.41	0.021	923	-	MF	17.41	CK ₀ D
URDD K ₀	0.1	1.50	1.29	0.012	923	-	DD	15.85	CK ₀ D
URMD HP	11.0	1.44	1.10	0.04	30027	1	MD	18.03	HP CID
URMF HP	11.1	1.52	1.17	0.05	30086	1	MF	17.77	HP CID

w_0 initial water content; v_0 initial specific volume; v_c specific volume after consolidation (before shearing); p_c' mean effective stress before shearing; γ_d dry density

Test type: CID: isotropically consolidated drained test; CIU: isotropically consolidated undrained test; CK₀D: K₀-consolidated drained test; CK₀U: K₀-consolidated undrained test; HP: High Pressure tests

Preparation method: DD: Dry deposition and hand Destructuration; MD: Moist tamping and hand Destructuration; SD: Slurry and hand Destructuration; MF: Moist tamping and Fines reconstitution

1

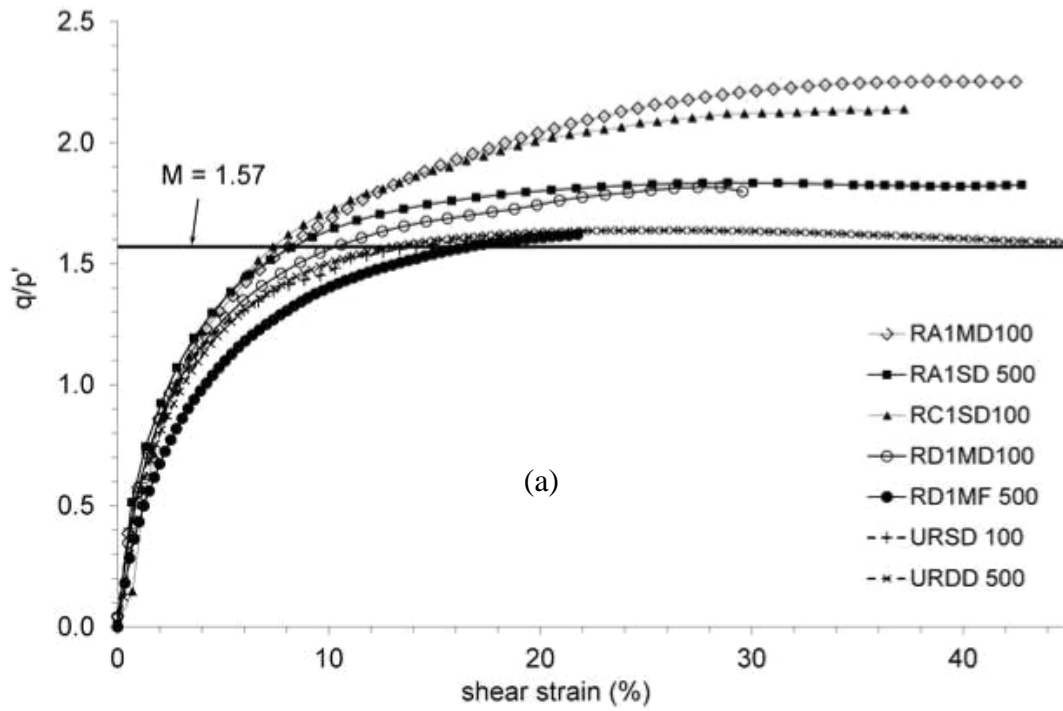
2

3 Table 2 Summary of the normal compression and critical state parameters for the reinforced

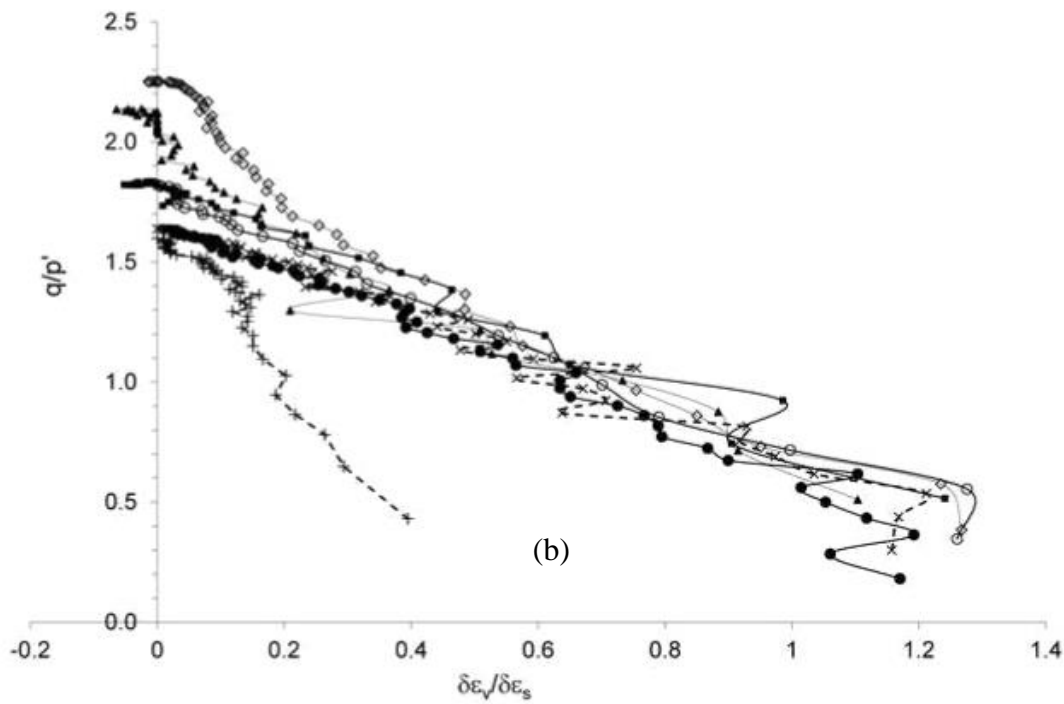
4 and unreinforced CDG

	Sample preparation	Isotropic NCL		CSL		
		λ	N	λ	Γ	M
Unreinforced CDG	D/M	0.061	1.73	0.061	1.69	1.57
	S/F	0.061	1.82	0.061	1.75	1.57
Reinforced CDG	All preparations	0.061	1.81	0.061	1.75	1.90

5



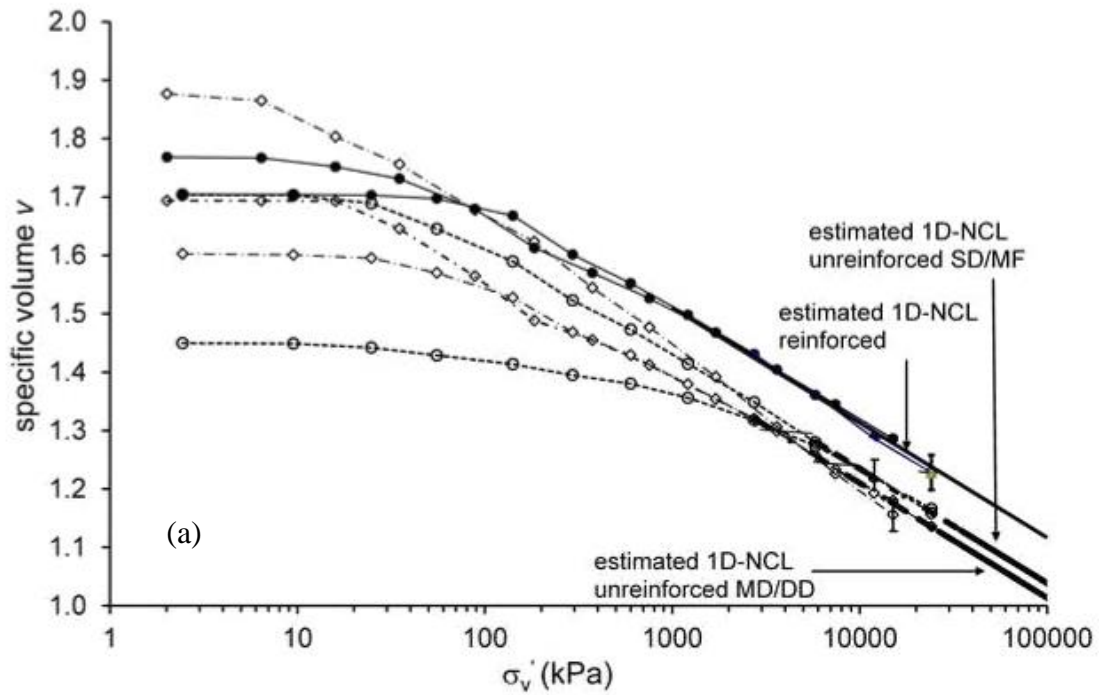
1



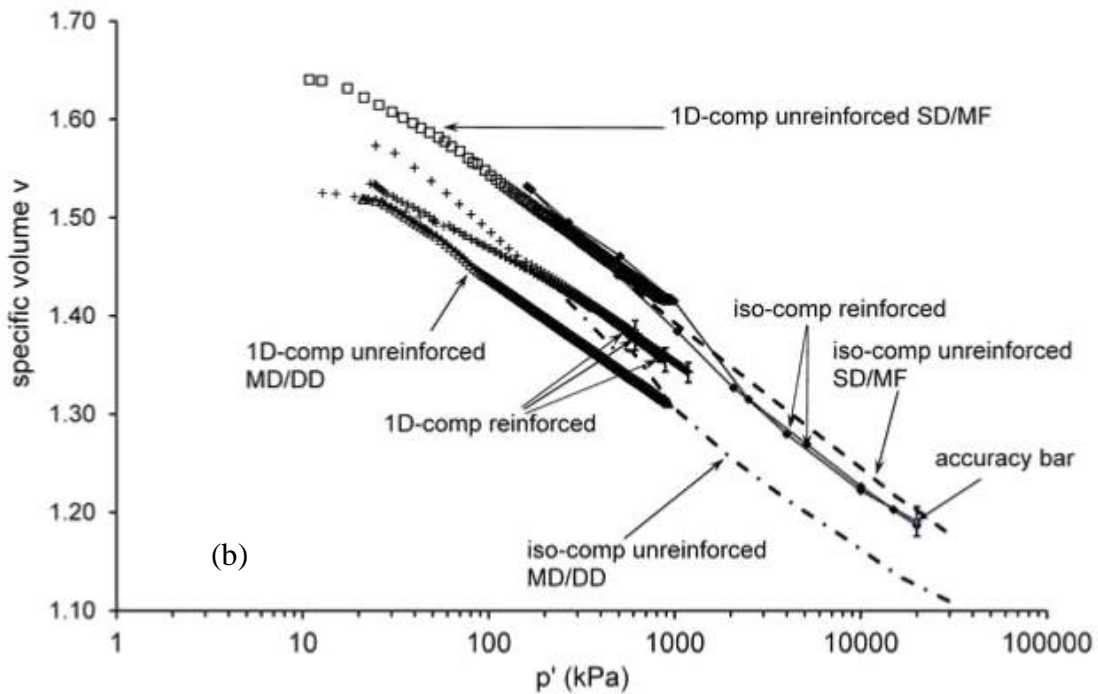
2

3 Figure 1- Determination of the optimum fiber-soil mixture form tests on CDG prepared with
 4 different fiber types and dosages (a) stress-strain response (b) stress dilatancy.

5



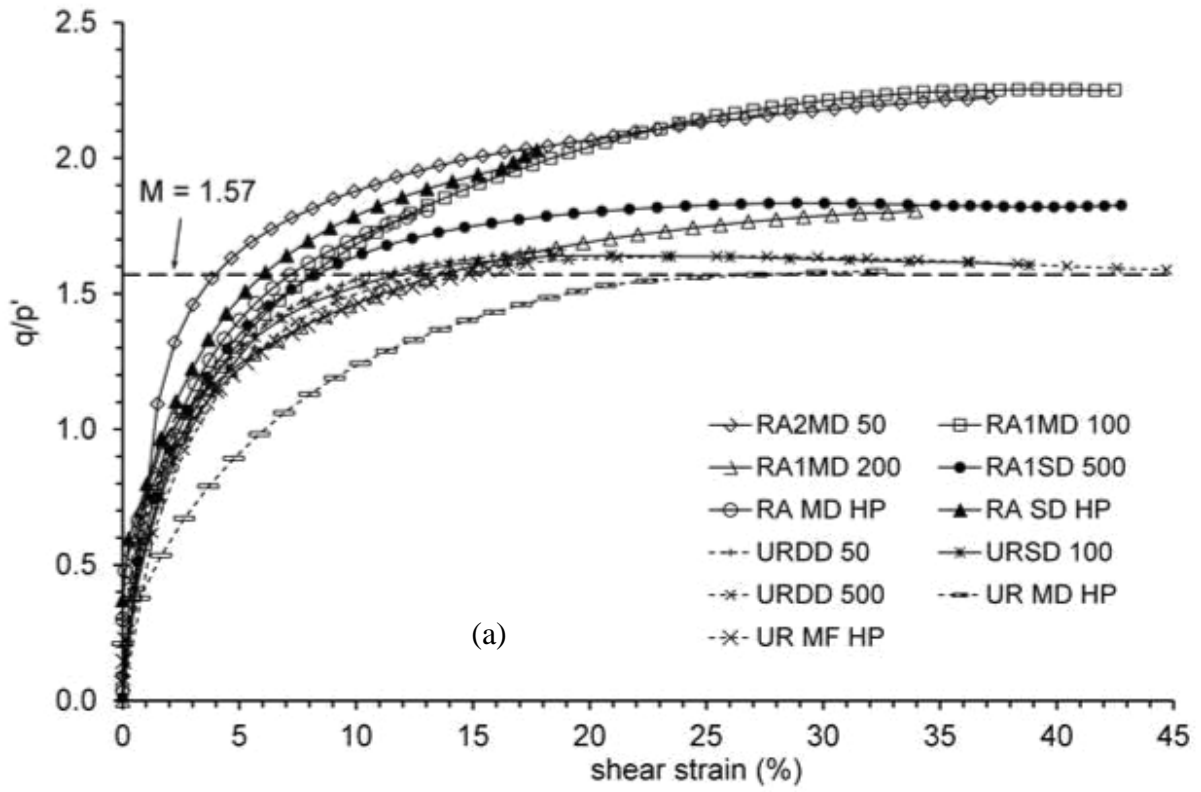
1



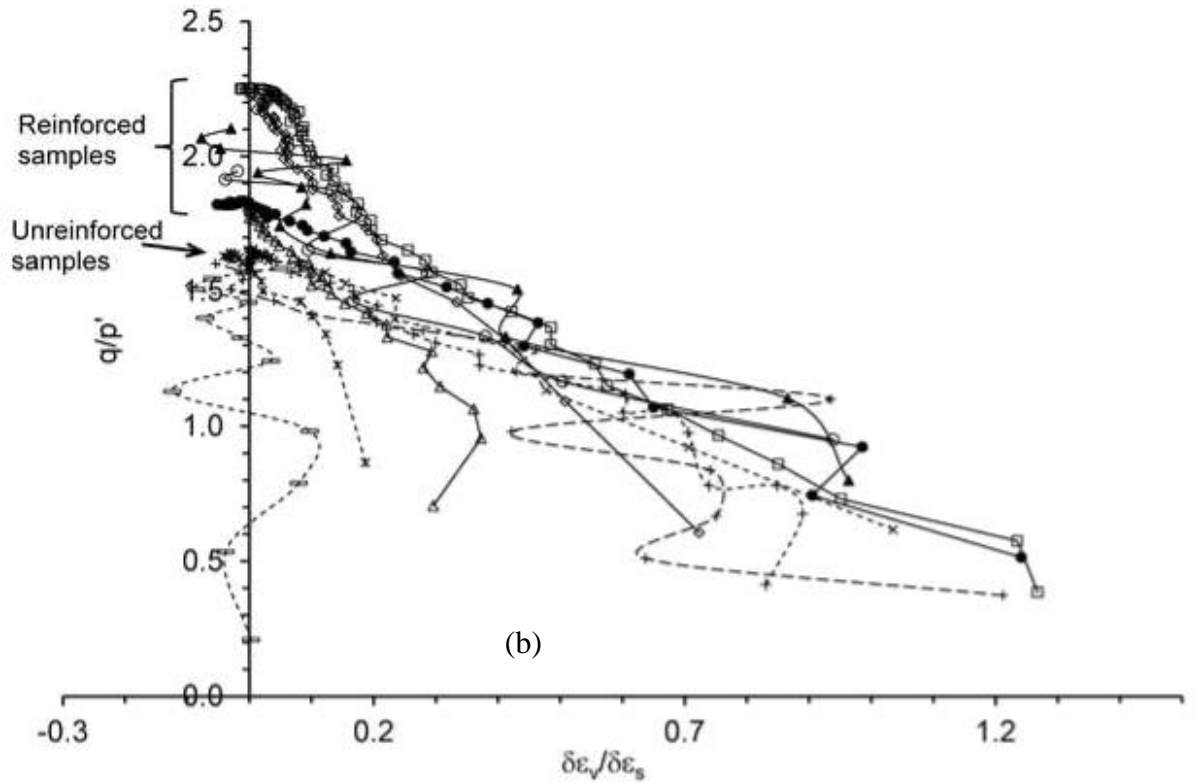
2

3 Figure 2 - (a) Oedometer and (b) triaxial one-dimensional and isotropic compression curves of
 4 reinforced and unreinforced CDG prepared with different methods. Unreinforced soil test data
 5 from Madhusudhan and Baudet (2014).

6



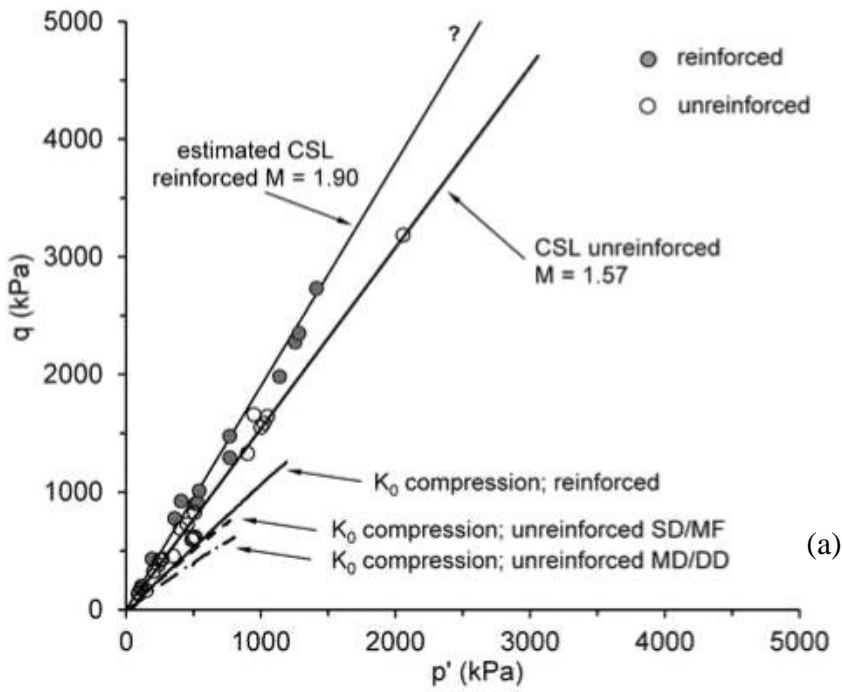
1



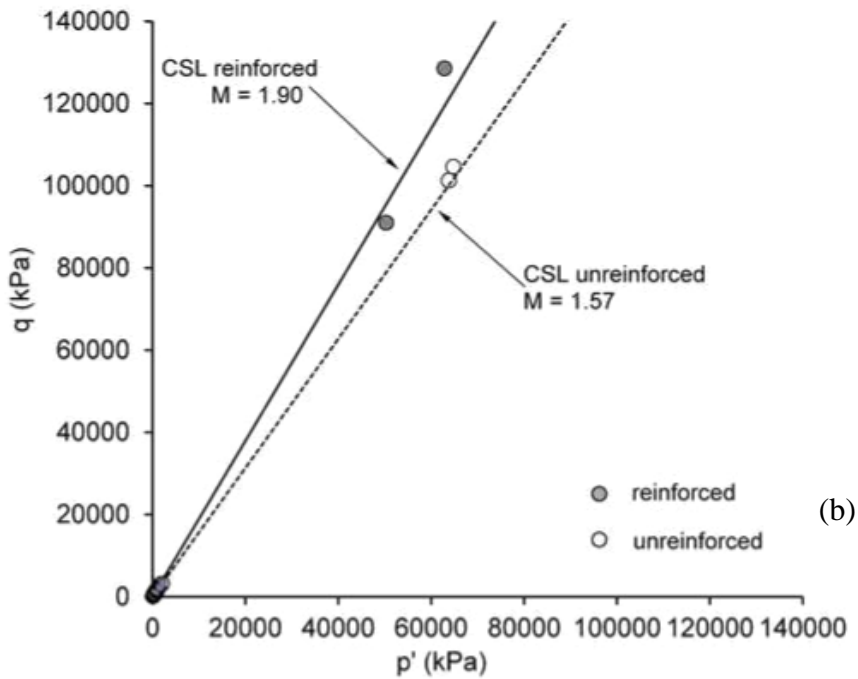
2

3 Figure 3 - Effect of material and sample preparation on the shearing behavior of CDG

4 reinforced with type-A fibers (a) stress-strain response (b) stress dilatancy



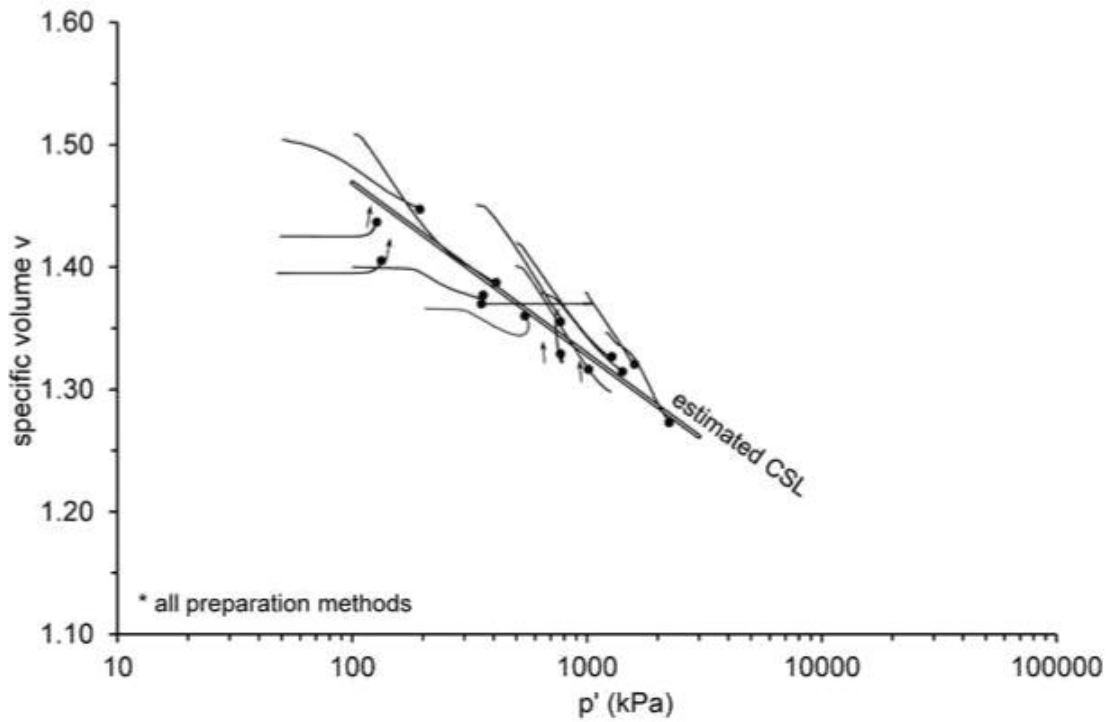
1



2

3 Figure 4 - Determination of the critical state line in (a) low to medium stress space (b) including
 4 the high pressure test data. The one-dimensional compression paths are also shown.

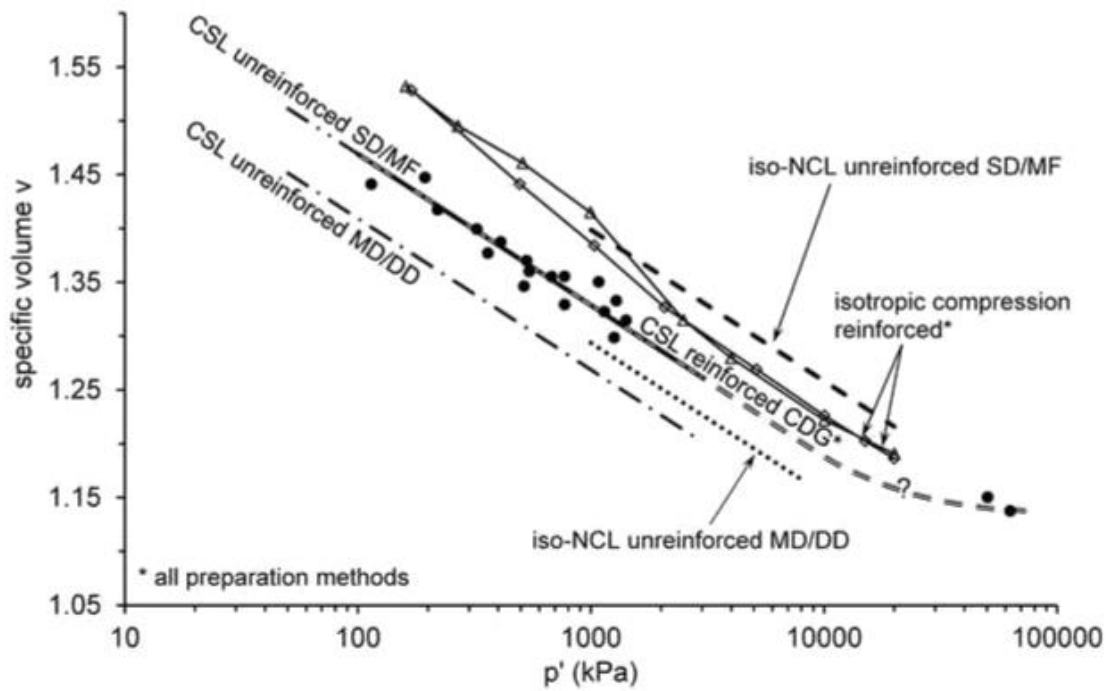
5



1

2 Figure 5 - Determination of the CSL of CDG reinforced with type-A fibers in state space

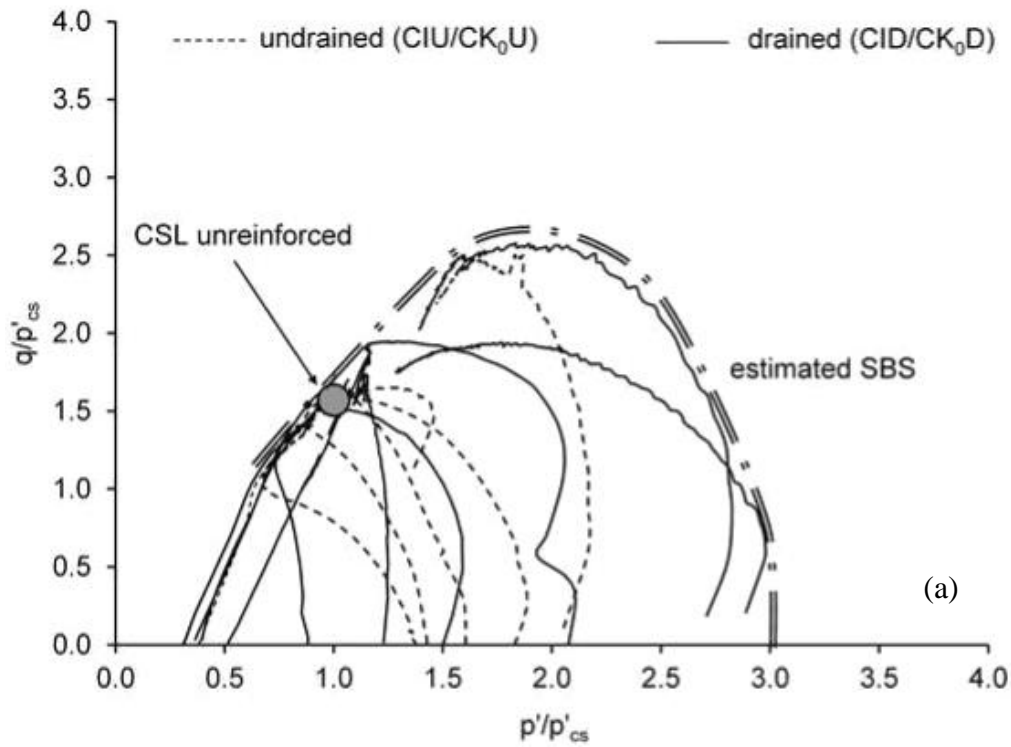
3



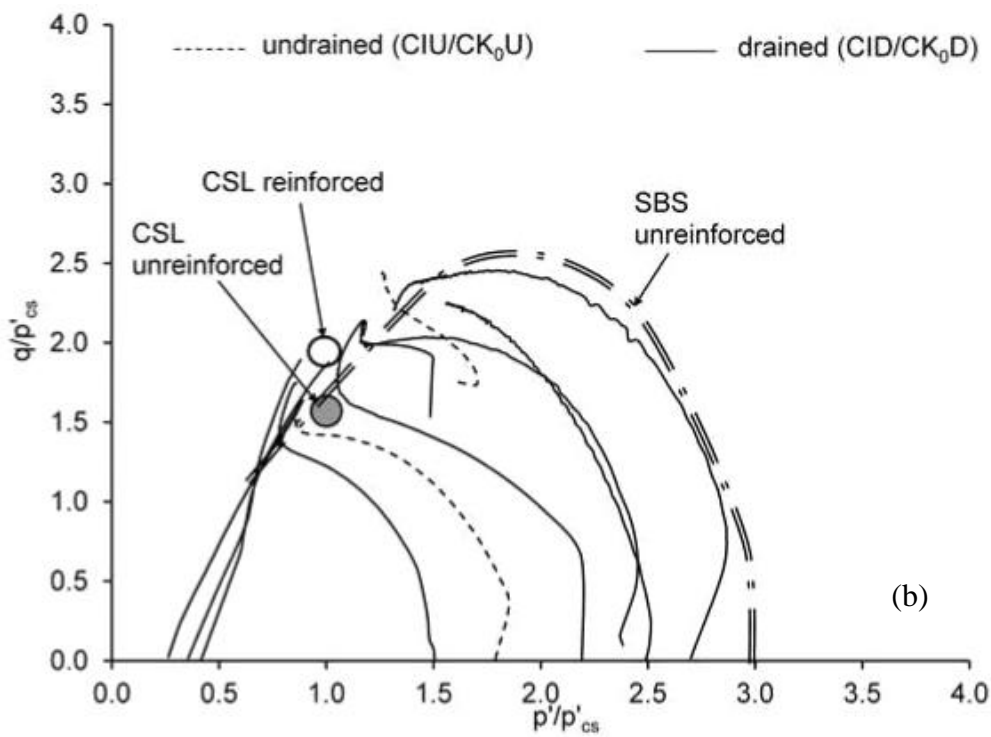
4

5 Figure 6 - Summary of normal compression and critical state lines obtained for the unreinforced

6 CDG and CDG reinforced with type-A fibers.

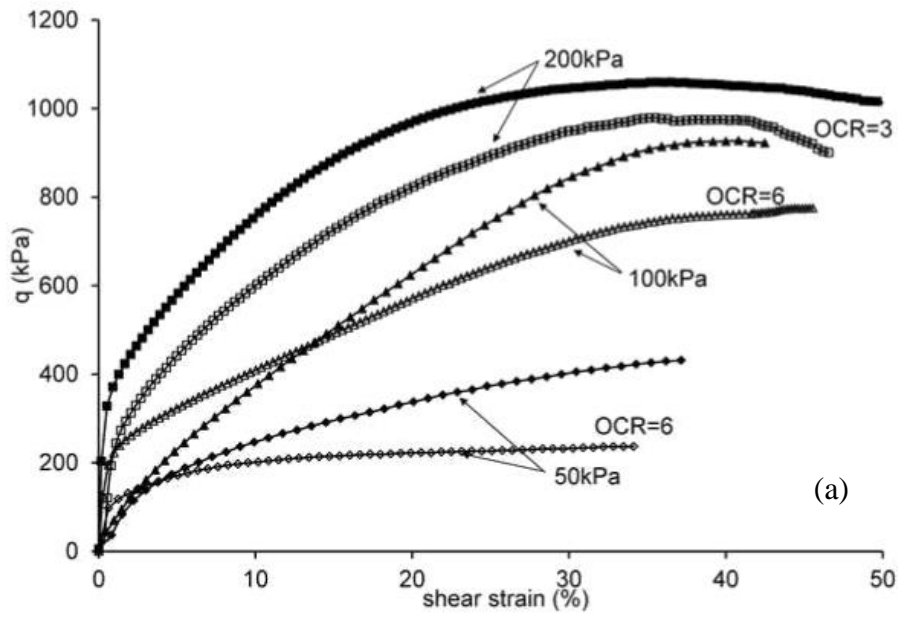


1

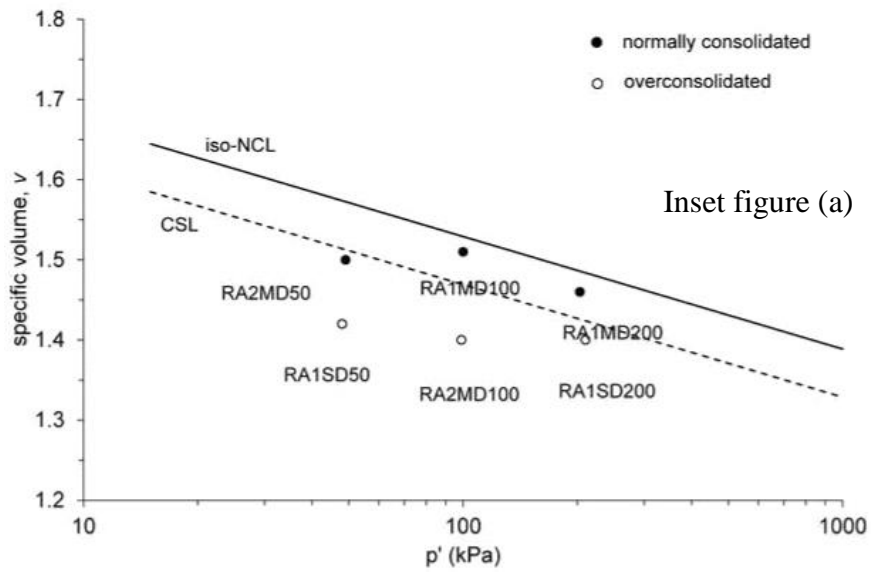


2

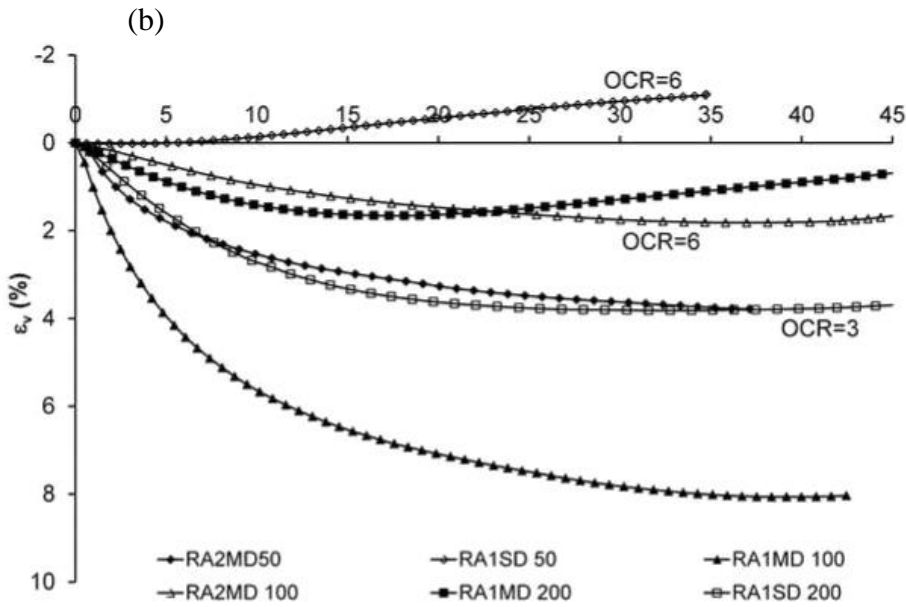
3 Figure 7 - State boundary surface of the (a) unreinforced CDG and (b) CDG reinforced with
 4 type-A fibers. The mean effective stresses have been normalized with respect to an equivalent
 5 pressure on the corresponding CSL.



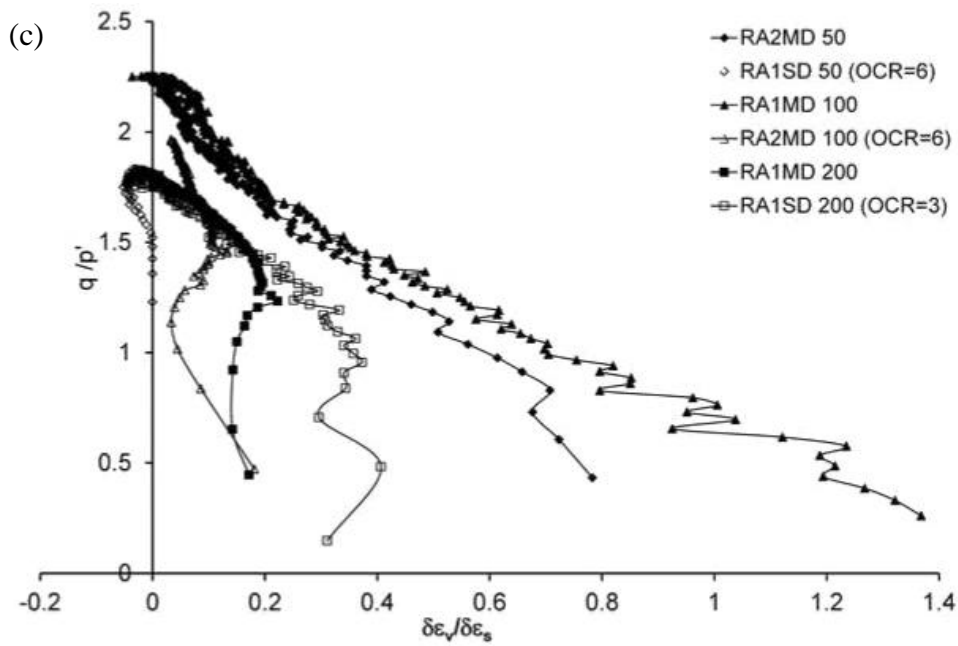
1



2



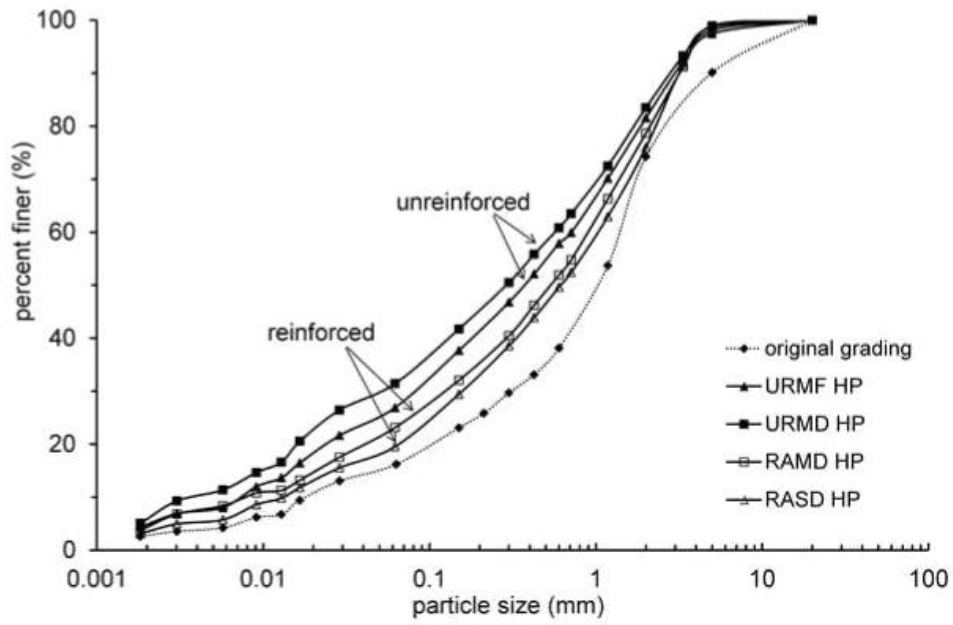
1



2

3 Figure 8 - Effect of overconsolidation on the (a) stress-strain response (inset critical state points
 4 on v - $\log p'$ space) (b) volumetric strain response and c) stress dilatancy of the type-A reinforced
 5 CDG.

6



1

2 Figure 9 - Effect of fibers on the amount of particle breakage during drained compression to

3 high pressure.